

A Homologous Series of Redox-Active, Dinuclear Cations with the Bridging Ligand 2-(2-Pyridyl)-1,8-naphthyridine

Cristian Saul Campos-Fernández, Xiang Ouyang, and Kim R. Dunbar*

Department of Chemistry, P.O. Box 30012, Texas A&M University, College Station, Texas 77842-3012

Received December 7, 1999

Extensive research has been devoted to metal complexes of nitrogen donor heterocyclic ligands because of their interesting luminescent properties.^{1–4} In considering the choices for metal building blocks to prepare assemblies with good electronic communication, one is struck by a general absence of those containing metal–metal bonds. Given the extensive redox chemistry exhibited by many dinuclear complexes and the possibility of coupling these units electronically, their incorporation into arrays is a promising new venue for the discovery of interesting optical and magnetic properties.⁵ In our quest for nitrogen heterocyclic ligands that are capable of spanning a dinuclear unit, we found several references on the use of cavity-shaped ligands such as 2-(2-pyridyl)-1,8-naphthyridine (pynp)^{6a–c} and 2,7-bis(2-pyridyl)-1,8-naphthyridine (bpnp)^{6a,d–g} (Figure 1).⁶ Among the compounds that were reported is [Rh₂(O₂CCH₃)₂(pynp)₂]²⁺, a molecule that exhibits intense low-energy optical transitions and a rich electrochemistry.^{6b} Despite the promising electronic properties of this compound, no additional examples of M–M bonded pynp derivatives have appeared in the literature and only one X-ray structure has been performed.^{6c} Herein we report the syntheses, electronic properties, and X-ray structures of the homologous series [M₂(O₂CCH₃)₂(pynp)₂]²⁺ (M = Mo, Ru, and Rh).

The starting materials [Mo₂(O₂CCH₃)₂(CH₃CN)₆][BF₄]₂,^{7,8} [Rh₂(O₂CCH₃)₂(CH₃CN)₆][BF₄]₂,⁷ and Ru₂(O₂CCH₃)₂Cl⁹ were reacted with pynp in a 2:1 ratio.^{6a} The reactions proceed with displacement of the equatorial acetonitrile ligands the Mo₂ and Rh₂ compounds and a loss of two acetate ligands accompanied by a one-electron reduction in the case of the Ru₂ complex.¹⁰

Compounds 1–3 were characterized by single-crystal X-ray studies,¹¹ cyclic voltammetry, ¹H NMR spectroscopy, and elec-

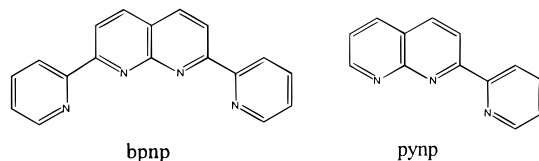


Figure 1. Schematic drawings of 2-(2-pyridyl)-1,8-naphthyridine (pynp) and 2,7-di(2-pyridyl)-1,8-naphthyridine (bpnp).

tronic spectroscopy. Crystals of [Mo₂(O₂CCH₃)₂(pynp)₂][BF₄]₂·3CH₃CN (**1**·3CH₃CN) and [Rh₂(O₂CCH₃)₂(pynp)₂][BF₄]₂·C₇H₈ (**2**·C₇H₈) were obtained after 1 week of slow diffusion of toluene into the reaction solutions. Single crystals of [Ru₂(O₂CCH₃)₂(pynp)₂][PF₆]₂·2CH₃OH (**3**·2CH₃OH) were obtained by layering the reaction solution with toluene that contained an excess of [*n*-Bu₄N][PF₆]. A representative thermal ellipsoid plot of the Mo₂ compound provided in Figure 2 illustrates that the dimetal units in these cations are spanned by two cis, tridentate pynp ligands and two bridging acetates. The tendency for naphthyridine to act as a bridge dominates this chemistry, but it should be pointed out that pynp can act as a chelating bipyridyl ligand to a single metal ion as found in the tris-substituted compound [Rh₂(pynp)₃Cl₂]²⁺.^{6c}

In all three dimetal cations, there is considerable distortion from linearity of the axial M–M–pyridyl interactions as evidenced by the M–M–N_{ax} angles of 169.6(3)° for Rh, 163.7(2)° for Ru, and 159.01[2]° for Mo. The pseudoaxial pyridine interactions are 2.206(9), 2.237(7), and 2.439[8] Å for Rh, Ru, and Mo, respectively; this trend is consistent with previous observations that the trans effect of a M–M single bond is much less than that of a double or a quadruple bond.^{7,12} As usual, the M–N_{eq}

- (1) Sutin, N.; Creutz, C. *Pure Appl. Chem.* **1980**, *52*, 2717.
- (2) Gilbert, J.; Eggleston, D.; Murphy, W.; Geselowitz, D.; Gersten, S.; Hodgson, D.; Meyer, T. *J. Am. Chem. Soc.* **1985**, *107*, 3855.
- (3) Binamira-Soriaga, E.; Sprouse, S.; Watts, R.; Kaska, W. *Inorg. Chim. Acta* **1984**, *84*, 135.
- (4) Declouire, Y.; Thummel, R. *Inorg. Chim. Acta* **1987**, *128*, 245.
- (5) (a) Cotton, F. A.; Lin, C.; Murillo, C. A. *J. Chem. Soc., Dalton Trans.* **1998**, 3151. (b) Wesemann, J. L.; Chisholm, M. H. *Inorg. Chem.* **1997**, *36*, 3258. (c) Cayton, R. H.; Chisholm, M. H.; Huffman, J. C.; Lobkovsky, E. B. *J. Am. Chem. Soc.* **1991**, *113*, 8709.
- (6) (a) Caluwe, P.; Evens, G. *Macromolecules* **1979**, *12*, 803. (b) Tikkanen, W.; Binamira-Soriaga, E.; Kaska, W.; Ford, P. *Inorg. Chem.* **1984**, *23*, 141. (c) Baker, A.; Tikkanen, W.; Kaska, W.; Ford, P. *Inorg. Chem.* **1984**, *23*, 3254. (d) Tikkanen, W.; Binamira-Soriaga, E.; Kaska, W.; Ford, P. *Inorg. Chem.* **1983**, *22*, 1147. (e) Thummel, R. P.; Lefoulon, F.; Williamson, D.; Chavan, M. *Inorg. Chem.* **1986**, *25*, 1675. (f) Binamira-Soriaga, E.; Keder, N. L.; Kaska, W. C. *Inorg. Chem.* **1990**, *29*, 3167. (g) Collin, J.-P.; Jouaiti, A.; Sauvage, J.-P.; Kaska, W. C.; McLoughlin, M. A.; Keder, N. L.; Harrison, W. T. A.; Stucky, G. D. *Inorg. Chem.* **1990**, *29*, 2238.
- (7) Pimblett, G.; Garner, D.; Clegg, W. *J. Chem. Soc., Dalton Trans.* **1986**, 1257.
- (8) Cotton, A.; Reid, A.; Schwotzer, W. *Inorg. Chem.* **1985**, *24*, 3965.
- (9) Martin, D.; Newman, R.; Vlasnik, L. *Inorg. Chem.* **1980**, *19*, 3404.
- (10) Compound **1**. ¹H NMR spectrum in CD₃CN at 25 °C: δ 9.05 (d, pynp), 8.85 (dd, pynp), 8.68 (d), 8.2 (td, pynp), 7.72 (m, pynp), 7.66 (m, pynp), 7.52 (m, pynp), 2.65 (s, CH₃-acetates). Compound **2**. ¹H NMR spectrum in CD₃CN at 25 °C: δ 9.70 (d, pynp), 8.87 (dd, pynp), 8.70 (d, pynp), 8.60 (m, pynp), 8.45 (dd, pynp), 8.35 (td, pynp), 7.48 (q, pynp), 2.25 (s, CH₃-acetate). Compound **3**. ¹H NMR signals were broad and featureless, which is indicative of paramagnetism.

- (11) **1**·3CH₃CN. Monoclinic, *P*2₁/*c*, *a* = 15.134(5) Å, *b* = 14.301(6) Å, *c* = 19.990(6) Å, β = 108.06(2)°, *V* = 4113(3) Å³, *Z* = 4, *d*_{calc} = 1.649 g/cm³, and μ (Mo Kα) = 0.697 mm⁻¹. A Rigaku AFC6S diffractometer was used to collect a hemisphere of data in the range 2.01 ≤ θ ≤ 24.98 at -100 ± 1 °C. The data were solved by direct methods in SHELXTL 5.0. All non-hydrogen atoms were refined anisotropically, and hydrogen atoms were calculated at fixed positions. Final least-squares refinement was based on 550 parameters and 7200 data points to give *R* = 0.0598 and *R*_w = 0.1690 and a goodness-of-fit of 1.017. A final difference Fourier map revealed the highest peak in the difference map to be 1.797 e⁻/Å³. **2**·C₇H₈. Monoclinic, *C*2/*c*, *a* = 13.408(2) Å, *b* = 21.670(3) Å, *c* = 13.726(2) Å, β = 94.865(2)°, *V* = 3973.9(8) Å³, *Z* = 4, *d*_{calc} = 1.685 g/cm³, and μ (Mo Kα) = 0.916 mm⁻¹. A hemisphere of data in the range 1.79 ≤ θ ≤ 24.72 was collected on a Siemens SMART 1K CCD area detector instrument at -140 ± 1 °C. The data were solved by direct methods in SHELXTL 5.0. All non-hydrogen atoms were refined anisotropically, and hydrogen atoms were calculated in fixed positions. Final least-squares refinement of 242 parameters and 3203 data points resulted in *R* = 0.1062 and *R*_w = 0.2365 and a goodness-of-fit of 1.117. A final difference Fourier map revealed the highest peak to be 1.377 e⁻/Å³. **3**·C₇H₈. Monoclinic, *C*2/*c*, *a* = 14.2228(7) Å, *b* = 20.3204(9) Å, *c* = 14.1022(7) Å, β = 95.144(1)°, *V* = 4059.3(3) Å³, *Z* = 8, *d*_{calc} = 1.808 g/cm³, and μ (Mo Kα) = 0.931 mm⁻¹. A hemisphere of data was collected on a Siemens SMART 1K CCD area detector instrument at -100 ± 1 °C in the range 1.75 ≤ θ ≤ 24.71 and solved by direct methods in SHELXTL 5.0. All non-hydrogen atoms were refined anisotropically, and hydrogen atoms were calculated at fixed positions. Final least-squares refinement of 294 parameters and 3429 data points resulted in *R* = 0.0617 and *R*_w = 0.1700 and a goodness-of-fit of 1.078. A final difference Fourier map revealed the highest peak to be 0.952 e⁻/Å³.

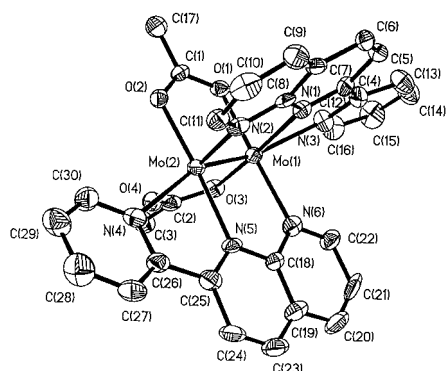


Figure 2. Thermal ellipsoid plot at the 50% level of the cation in $[\text{Mo}_2(\text{O}_2\text{CCH}_3)_2(\text{pynp})_2][\text{BF}_4]_2 \cdot 3\text{CH}_3\text{CN}$ (**1**· $3\text{CH}_3\text{CN}$).

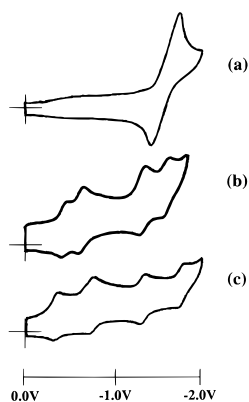


Figure 3. Cyclic voltammograms of (a) the pynp ligand, (b) $[\text{Mo}_2(\text{O}_2\text{CCH}_3)_2(\text{pynp})_2][\text{BF}_4]_2 \cdot 3\text{CH}_3\text{CN}$, and (c) $[\text{Ru}_2(\text{O}_2\text{CCH}_3)_2(\text{pynp})_2][\text{PF}_6]_2 \cdot \text{CH}_3\text{OH}$ at a Pt electrode vs Ag/AgCl in 0.1 M TBAH/CH₃CN.

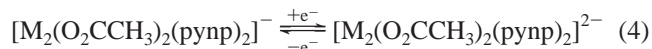
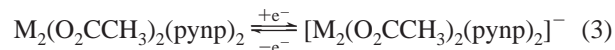
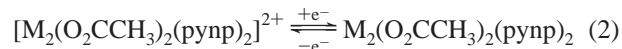
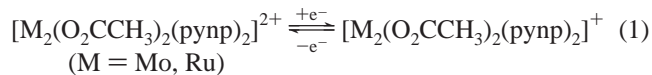
interactions are considerably shorter than the M–N_{ax} bonds; the averages are 2.018[11] Å for Rh, 2.072[5] Å for Ru, and 2.211–[8] Å for Mo. A quantitative assessment of the trans effect of the metal–metal bond is the difference [(M–N_{ax}) – (M–N_{eq})], which is 0.188, 0.189, and 0.165 Å for the Rh₂, Ru₂, and Mo₂ compounds, respectively. The metal–metal bond distances of 2.124(1), 2.298(1), and 2.407(2) Å are in the expected ranges for Mo–Mo quadruple (~2.0–2.2 Å), Ru–Ru double (~2.2–2.4 Å), and Rh–Rh single (2.35–2.45 Å) bonds, respectively.¹²

The electronic spectral properties of the compounds were measured in acetonitrile solution. $[\text{Mo}_2(\text{O}_2\text{CCH}_3)_2(\text{pynp})_2]^{2+}$ exhibits two transitions in the visible region, one at 432 nm ($\epsilon = 1.8 \times 10^3 \text{ M}^{-1} \text{ cm}^{-1}$) and a second feature at 857 nm ($\epsilon = 4.75 \times 10^2 \text{ M}^{-1} \text{ cm}^{-1}$). $[\text{Rh}_2(\text{O}_2\text{CCH}_3)_2(\text{pynp})_2]^{2+}$ exhibits transitions at 355 nm ($\epsilon = 8.7 \times 10^3 \text{ M}^{-1} \text{ cm}^{-1}$) and 451 nm ($\epsilon = 2.4 \times 10^3 \text{ M}^{-1} \text{ cm}^{-1}$), and $[\text{Ru}_2(\text{O}_2\text{CCH}_3)_2(\text{pynp})_2]^{2+}$ exhibits two transitions at 327 nm ($\epsilon = 3.4 \times 10^4 \text{ M}^{-1} \text{ cm}^{-1}$) and 671 nm ($\epsilon = 3.6 \times 10^4 \text{ M}^{-1} \text{ cm}^{-1}$). The intense optical transitions located at lower energies in these complexes are not present in spectra of the parent tetracarboxylate compounds.¹² These differences are attributed to the presence of the “noninnocent” pynp ligands that participate in MLCT transitions.

Tetracarboxylate compounds of the lantern type $\text{M}_2(\text{O}_2\text{CCH}_3)_4$ (M = Mo,^{13a} Rh,^{13b} Ru^{13c}) exhibit unremarkable redox properties characterized by one reversible oxidation and, in the case of the Rh and Ru analogues, an irreversible metal-based reduction. In contrast, cyclic voltammetric studies reveal a rich redox chemistry for $[\text{M}_2(\text{O}_2\text{CCH}_3)_2(\text{pynp})_2]^{2+}$ compounds. The cyclic voltammogram of $[\text{Mo}_2(\text{O}_2\text{CCH}_3)_2(\text{pynp})_2][\text{BF}_4]_2$ contains four reversible

reductions at $E_{1/2}^{(1)} = -0.43 \text{ V}$, $E_{1/2}^{(2)} = -0.67 \text{ V}$, $E_{1/2}^{(3)} = -1.34 \text{ V}$, and $E_{1/2}^{(4)} = -1.66 \text{ V}$ and an irreversible oxidation at $E_{p,a} = 0.86 \text{ V}$. The second reduction occurs at a potential that is 240 mV more positive than the first couple, and the third and fourth couples are separated by 320 mV. These $\Delta E_{1/2}$ values correspond to comproportionation constants, K_c , of 1.2×10^4 and 2.70×10^5 , respectively. These values are in the range reported for partially delocalized systems, or class II according to the Robin–Day classification.¹⁴ $[\text{Ru}_2(\text{O}_2\text{CCH}_3)_2(\text{pynp})_2][\text{PF}_6]_2$ also exhibits four one-electron, reversible reductions located at $E_{1/2}^{(1)} = -0.43 \text{ V}$, $E_{1/2}^{(2)} = -0.82 \text{ V}$, $E_{1/2}^{(3)} = -1.40 \text{ V}$, and $E_{1/2}^{(4)} = -1.84 \text{ V}$. The second reduction is shifted to more positive potentials by 390 mV with respect to the first process. This separation corresponds to $K_c = 3.9 \times 10^6$, which means that the unpaired electron is delocalized over the two pynp ligands (class III Robin–Day behavior).¹³ The third and fourth reductions occur at a separation of 420 mV ($K_c = 2.7 \times 10^7$; class III). In contrast to the other two compounds, the electrochemistry of $[\text{Rh}_2(\text{O}_2\text{CCH}_3)_2(\text{pynp})_2][\text{BF}_4]_2$ consists of a quasi-reversible reduction at $E_{1/2} = -0.58 \text{ V}$ and an irreversible wave at $E_{p,c} = -1.08 \text{ V}$ with an associated chemical return wave at $E_{p,a} = -0.80 \text{ V}$. A number of ill-defined irreversible features are also present at more negative potentials.

The new homologous series presented here allows one to make comparisons of compounds with different metal frontier orbitals. Cyclic voltammetric data indicate that all four of the one-electron reduction products are stable for Mo₂ and Ru₂, including the mixed-valence intermediates $[\text{M}_2(\text{O}_2\text{CCH}_3)_2(\text{pynp})_2]^+$ and $[\text{M}_2(\text{O}_2\text{CCH}_3)_2(\text{pynp})_2]^-$ (eqs 1 and 3). Conversely, there are no stable



reduction products of $[\text{Rh}_2(\text{O}_2\text{CCH}_3)_2(\text{pynp})_2]^{2+}$. One possible explanation for these differences is the fact that delocalization of the naphthyridine π system of pynp through the Mo₂⁴⁺ or Ru₂⁴⁺ units can occur via empty δ^* and π^* LUMO's on Mo₂ and Ru₂, respectively. In the case of the dirhodium complex, however, the only available metal orbital is σ^* , which is not of the appropriate symmetry to interact with the ligand π system.

Acknowledgment. We gratefully acknowledge NSF for providing financial support and Dr. Donald Ward for help with aspects of the X-ray crystallographic studies.

Supporting Information Available: Tables listing detailed crystallographic data, atomic positional parameters, and bond lengths and angles and ORTEP plots of compounds **2**· $2\text{CH}_3\text{OH}$ and **3**· C_4H_8 . This material is available free of charge via the Internet at <http://pubs.acs.org>.

IC991406J

- (13) (a) Zietlow, T. C.; Klendworth, D. D.; Nimry, T.; Salmon, D. J.; Walton, R. A. *Inorg. Chem.* **1981**, *20*, 947. (b) Das, K.; Kadish, K. M.; Bear, J. L. *Inorg. Chem.* **1978**, *17*, 930. (c) Lindsay, A. J.; Wilkinson, G.; Motevalli, M.; Hursthouse, M. B. *J. Chem. Dalton Trans.* **1985**, 2321. (d) Carvill, A.; Higgins, P.; McCann, G. M.; Ryan, H.; Shields, A. J. *Chem. Soc., Dalton Trans.* **1989**, 2435.

- (14) Robin, M. B.; Day, P. *Adv. Inorg. Chem. Radiochem.* **1967**, *10*, 247.

(12) Cotton, F. A.; Walton, R. A. *Multiple Bonds Between Metal Atoms*, 2nd ed.; Clarendon Press: Oxford, 1993.